PAPER: Classical statistical mechanics, equilibrium and non-equilibrium

Random sequential adsorption of polydisperse mixtures on a cubic lattice

M Beljin-Čavić[1], Lj Budinski-Petković[1], I Lončarević[1,*], Z M Jakšić[2] and S B Vrhovac[2]

[1] Faculty of Technical Sciences, University of Novi Sad, Trg D. Obradovića 6, Novi Sad 21000, Serbia
[2] Institute of Physics Belgrade, University of Belgrade, Pregrevica 118, Zemun 11080 Belgrade, Serbia
E-mail: ivanalon@uns.ac.rs

Abstract. The irreversible random sequential adsorption of polydisperse mixtures of 'lattice animals' on a three-dimensional cubic lattice is investigated using Monte Carlo simulations. A 'lattice animal' is defined as a 3D object composed of a group of points connected as nearest neighbors on a lattice. Polydisperse mixtures consist of n objects of varying sizes but sharing the same basic shape. This study analyzes the influence of polydispersity and the geometrical properties of the shapes on the jamming density θ_{J} and the temporal evolution of the density $\theta(t)$. The approach of the coverage to the jamming limit θ_{J} is found to be exponential, expressed as $\theta(t) = \theta_{\mathrm{J}} - A\mathrm{e}^{-t/\sigma}$, both for the mixtures and their individual components. The values of relaxation time σ are determined by the number of different orientations m that the lattice animals can take when placed on a cubic lattice. It is observed that the parameter σ increases linearly with the number of mixture components n of the same basic shape. Additionally, the partial jamming densities and corresponding relaxation times σ decrease as the size of the mixture components increases.

Keywords: irreversible deposition, 'lattice animals', 3D lattice, jamming coverage

---

*Author to whom any correspondence should be addressed.

Contents

1. Introduction

Packings consisting of various objects are of great scientific and technological importance, ranging from agriculture, ecology, biology, material science, nanotechnology [1–8], etc. Depositing objects could be granular particles, polymer chains, globular proteins, DNA segments, nanoparticles, such as nanotubes, nanoribbons, or nanoplates, making an inexhaustible research base. The packing structure is still not able to be predicted by a general model that takes into account various controlling parameters, such as geometric and material properties of objects. Describing the packing processes is among the most persistent problems in science [9].

Deposition processes where microscopic events occur essentially irreversibly on the time scales of interest are broadly studied as random sequential adsorption (RSA) on a lattice [10, 11]. The RSA model considers sequential addition of particles of various shapes at randomly chosen places on the D-dimensional substrate. Overlapping of the particles is not allowed, and there is no diffusion of the deposited objects. The kinetics of the deposition process are described by the time evolution of the coverage (or the density of the system), $\theta(t)$, that is the fraction of the substrate occupied by the deposited objects at time t. Once an object is placed, it affects the geometry of all later placements so that the dominant effect in RSA is the blocking of the available substrate space. At sufficiently large times the coverage $\theta(t)$ approaches the jamming value θ_{J}, where only gaps too small to place new particles are left on the substrate and the limiting (jamming) coverage θ_{J} is less than the corresponding density of closest packing.

Depending on the system of interest, RSA models can differ in substrate dimensionality, while the substrate can be continuum or discrete. Analytical results are available mostly for one-dimensional problems [12]. Due to the complexity of deposition processes in higher dimensions, Monte Carlo simulations represent the main tool for describing such systems. The long-term behavior of the coverage fraction $\theta(t)$ is known to be

asymptotically algebraic in the case of continuum substrates [13, 14]. For the lattice model approach to jamming coverage, θ_J is exponential [15–17], of the form:

$$\theta(t) = \theta_J - A e^{-t/\sigma}. \tag{1}$$

The jamming coverage θ_J, the relaxation time σ, and the parameter A depend on the shape of depositing objects and their orientational freedom, on the substrate dimensionality, on the type of depositing particles (monodisperse or mixtures), and other specific conditions.

RSA models have been extensively studied during the last few decades. Influence of the particle shapes on the packing density was investigated for continuum [18–21] and discrete models [22–25]. Deposition of objects of various sizes and rotational symmetries that can be made by self-avoiding random walks on a triangular lattice was studied in [24]. It was found that shapes with the symmetry axis of a higher order have lower values of relaxation time σ, i.e. they approach their jamming limit more rapidly. The jamming coverage θ_J decreases with the object size regardless of their shape. Nevertheless, for sufficiently large objects it turns out that changing the shape has considerably more influence on the jamming density than increasing the object size. In the case of the RSA of lattice animals on a 3D cubic lattice [25] it was shown that the relaxation time σ is equal to the number of different orientations m that lattice animals can take when placed on a cubic lattice.

Real physical systems often consist of polydisperse particles, i.e. particles of different shapes and sizes. Irreversible deposition in polydisperse systems was studied for binary mixtures [26–29], and for mixtures of particles obeying various size distributions [30–32]. Numerical simulations of the deposition of two-component mixtures of line segments on a square lattice [26] showed that the mixtures cover the lattice more efficiently than either of the species separately. RSA of polydisperse mixtures containing depositing objects of various shapes and sizes was studied by Monte Carlo simulations, and the mixtures were made of objects formed by self-avoiding random walks on a triangular lattice [33]. It was found that the symmetry properties of the objects have a decisive influence on the adsorption rate of each mixture component. Both the partial jamming coverage and the corresponding relaxation time decrease very rapidly with the size of the objects making the mixture. Jamming coverage for the mixture was found to increase with the number of components n for mixtures of more symmetric objects, contrary to the mixture of less symmetric objects where jamming coverage decreases.

Much attention has been paid to the RSA on 1D and 2D lattices, but there are significantly fewer studies of irreversible deposition in 3D [25, 34, 35]. In this paper, we present the results of Monte Carlo simulations for the irreversible RSA of polydisperse mixtures of lattice animals on a 3D cubic lattice. RSA of lattice animals on 3D lattices is a complex problem in itself. Introducing polydispersity increases the complexity of the studied systems, and the aim of this work is to investigate these processes in a systematic way.

The paper is organized as follows. Section 2 describes the model and the details of the simulations. The kinetics of the process and the dependence of the jamming coverage on

the number of mixture components are analyzed in section 3. Finally, section 4 contains some additional comments.

2. Definition of the model and the simulation method

Depositing objects are 'lattice animals' which are connected graphs on a grid. A *site* animal can be seen as a finite set of lattice sites connected by nearest-neighbor bonds. In mathematics, and particularly in combinatorics, the terms polyominoes and polycubes are commonly used. A polyomino of size N is an edge-connected set of N squares on the square lattice. A polycube of size N is a face-connected set of N cubes in the cubic lattice. Since the square (cubic) lattice is self-dual, polyominoes (polycubes) are equivalent to *site* animals on the dual lattice.

Lattice animals can be categorized as 'fixed' or 'free'. 'Fixed' lattice animals are considered different if they have different shapes or orientations. On the other hand, 'free' lattice animals are distinguished only by shape, not by orientation. Fixed polycubes are most commonly discussed in the context of enumeration, which determines the number of polycubes corresponding to a specific parameter, usually their size or perimeter. There is no known analytic formula for calculating the number of fixed D-dimensional polycubes of size N, $A_d(N)$, $d > 1$. The only known methods for computing $A_d(N)$ are based on enumerating all the polyominoes or polycubes using various numerical algorithms [36, 37].

In this work, we focus on the 'free' lattice animals on a 3D cubic lattice. The term 'free' will be omitted in the following text. Lunnon [38] analyzed polycubes by considering the symmetry groups and computed the number of 3D polycubes of size up to $N = 6$. Most polycubes are asymmetric, but many have more complex symmetry groups. A polycube without symmetry has 24 different orientations. The number of orientations m that a polycube may take varies with the symmetry of the polycube. There are seven classes of lattice animals with different numbers of possible orientations on a cubic lattice, and the corresponding values of the parameter m are $m \in \{1, 3, 4, 6, 8, 12, 24\}$ [25].

Table 1 shows all polycubes of size $N = 1, 2, 3$, and 4 and equivalent lattice animals on the dual lattice. Polycubes of size $N = 1, 2, 3$ are planar with a maximum of 12 different orientations (object V3). There is only one shape of size $N = 1$ (monomer (M)), and also one shape of size $N = 2$ (dimer (D)). Three connected lattice sites can form two different lattice animals. There are eight tetracubes (fourth-order polycubes), five of which are planar. A tetracube A4 and its mirror image B4 (chiral twins) are considered distinct because there is no rigid motion that transforms one onto the other. Monomer has the lowest number ($m = 1$), while the shape (L4) has the highest number ($m = 24$) of possible orientations. An overview of all lattice animals of size $N \leqslant 5$ is given in our previous works [25, 39] (see, e.g. large tables 1 and 2 in [39]).

Polydisperse mixtures are composed of n objects of various sizes but of the same basic shape. The basic objects used for generating larger objects in simulations are the monomer (M), dimer (D), objects (V3), (A4), (L4), (O4), (P4), (S4), (T4), and the cubes (C8). Objects larger than the basic ones are created through isotropic scaling. Uniform scaling is a linear transformation that enlarges or shrinks objects by a scale

Table 1. Shown here are all polycubes of size $N = 1$, 2, 3, 4 together with the equivalent lattice animals (x) on the dual lattice. For each lattice animal (x) with m possible orientations, $\theta_{\mathrm{J}}^{(x)}$ is the jamming coverage. The numbers in parentheses are the numerical values of the standard uncertainty of $\theta_{\mathrm{J}}^{(x)}$ referred to the last digits of the quoted values.
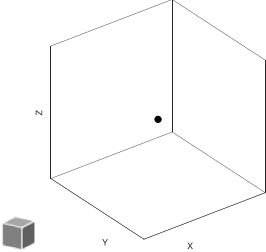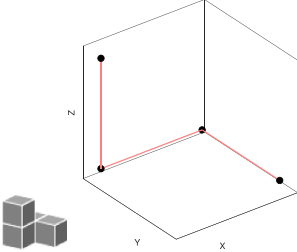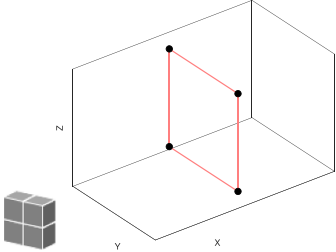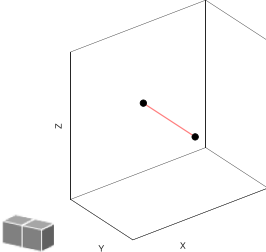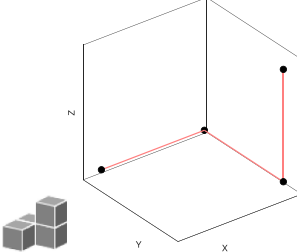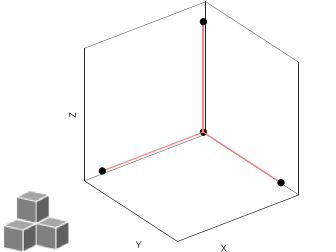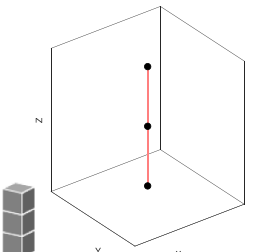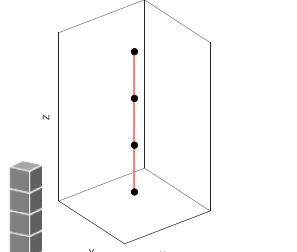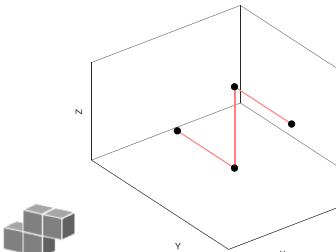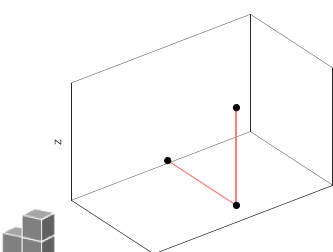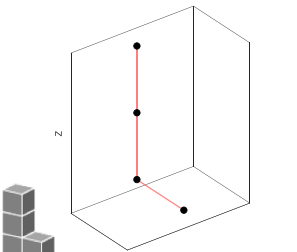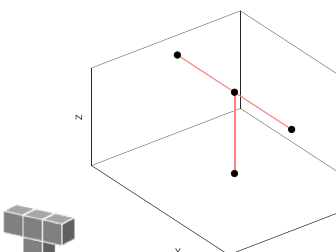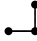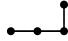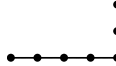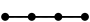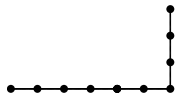
(x), m; $\theta_{\mathrm{J}}^{(x)}$	(x), m; $\theta_{\mathrm{J}}^{(x)}$	(x), m; $\theta_{\mathrm{J}}^{(x)}$
(M),1; 1.0000(0)	(A4),12; 0.8178(2)	(O4),3; 0.8079(3)
(D),3; 0.9184(1)	(B4),12; 0.8178(2)	(P4),8; 0.7941(3)
(I3),3; 0.8390(2)	(I4),3; 0.7808(3)	(S4),12; 0.8149(2)
(V3),12; 0.8788(2)	(L4),24; 0.8339(2)	(T4),12; 0.8114(3)

Table 2. Larger objects of the same shape are made by repeating each bond of the basic shape the same number of times, as illustrated for the k-mers, objects (V3), and (L4). Number of lattice sites occupied by the object is N.

(D)	N	(V3)	N	(L4)	N
•—•	2	⌐	3	⌐	4
•—•—•	3		5		7
•—•—•—•	4		7		10
...	...	...	...	...	...

factor that is the same in all directions. The results of uniform scaling are similar to the original. Similarity is a transformation that preserves angles and changes all distances in the same ratio, called the ratio of magnification r. Actually, objects of larger sizes than the basic ones are created in simulations by repeating each bond of the basic shape the same number of times r. The process of forming larger objects is illustrated in table 2 for k-mers and basic shapes (V3) and (L4). Objects created from the primary object (A4) by uniform scaling with factors $r = 1, 2, 3, 4$ are shown in figure 1. A polydisperse mixture with n components, corresponding to a chosen basic object (X), contains the basic object (X) and all objects similar to it obtained through isotropic scaling with scale factors $k = 2, \ldots, n$.

A mixture of objects of various shapes but the same size is made of objects covering four lattice sites from table 3.

The numerical algorithm used to deposit a lattice animal at randomly chosen places on the 3D substrate was already described in detail in previous papers [25, 39]. Therefore, we shall present it briefly, giving the algorithm additions necessary for mixture deposition. At each Monte Carlo step, a lattice site is selected randomly. If the chosen site is unoccupied, one of the objects making the mixture is selected at random, and deposition of the object is tried in one of the 24 possible orientations that are also chosen at random. Then, the head of the object is fixed at the selected site, and it is searched whether all necessary sites are unoccupied. If so, the object is placed, and the corresponding sites are denoted as occupied. If the attempt fails, then a new site, object, and orientation are selected randomly, and so on. The jamming density is reached when neither of the objects from the mixture can be placed in any position on the lattice. During the simulation, we record the total number of inaccessible sites in the lattice. Inaccessible sites include both occupied and unoccupied sites that cannot serve as the starting point for depositing the object in any of the 24 possible orientations. We determine that the jamming limit is reached when the number of inaccessible sites equals the total number of sites in the lattice. After each kL^3 attempt to deposit the object, we check this condition, starting from a later time point established in previous simulations on smaller lattices. Depending on the size of the object, the value of
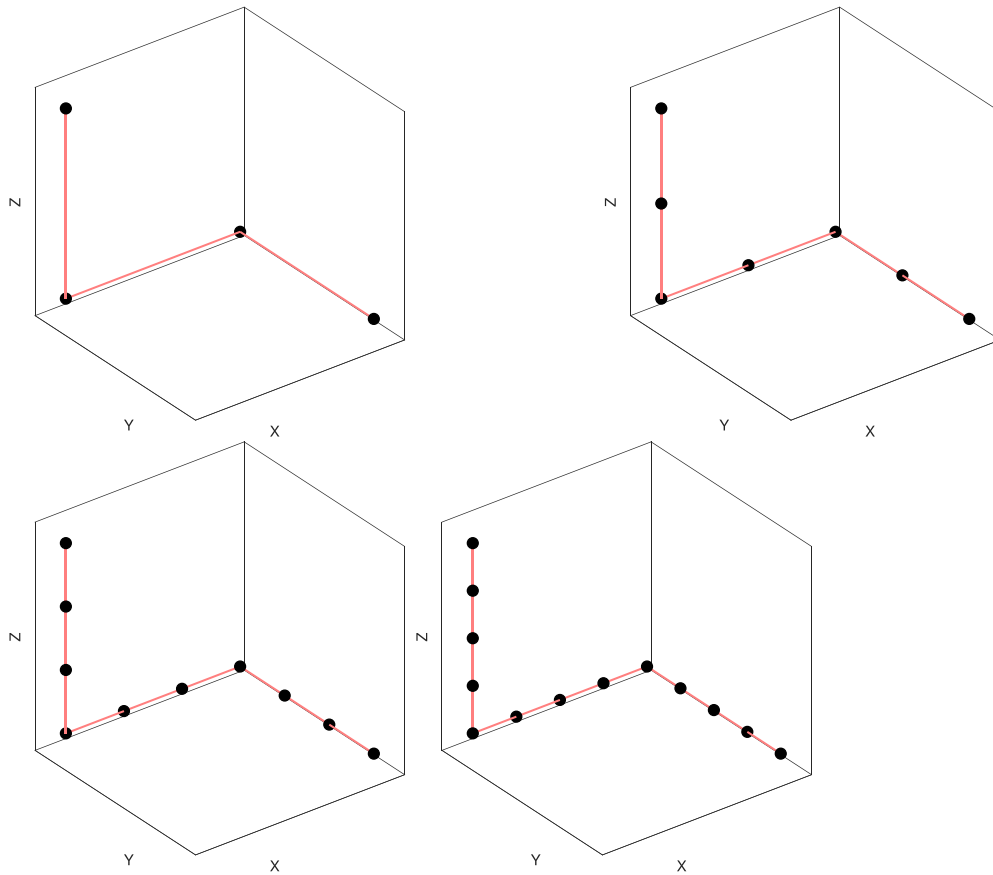
Figure 1. The process of forming larger objects from the primary object (A4) by uniform scaling with factors $r = 1, 2, 3, 4$.

Table 3. Relaxation time σ and the jamming density θ_{J} for objects of the same size but various shapes making the eight-component mixture. The objects are illustrated in table 1.

Shape	m	σ	θ_{J}
(A4)	12	90.99	0.1110
(B4)	12	90.66	0.1110
(I4)	3	18.59	0.1048
(L4)	24	191.20	0.1173
(O4)	3	19.24	0.1090
(P4)	8	62.97	0.1045
(S4)	12	90.58	0.1109
(T4)	12	90.74	0.1071
MIXTURE		184.84	0.8755

parameter k can be 20, 50 or 100. If this condition is met, we terminate the current simulation run and move on to the next one.

The Monte Carlo simulations are performed on a 3D cubic lattice of size $L = 128$. Periodic boundary conditions are used in all directions. The time is counted by the number of attempts to select a lattice site and scaled by the total number of lattice sites. The data are averaged over 100 independent runs for each of the investigated mixtures.

3. Results and discussion

The simulations were performed for mixtures containing n objects of different sizes, which were created by scaling the same base object. It is important to note that in each deposition attempt the objects are selected from the mixture with equal probability. We can imagine that we randomly choose one object from a large reservoir of objects containing all components of the mixture with equal fractional concentrations. At the same time, we assume that the fractional concentrations of the mixture components in the reservoir do not change due to adsorption events. Number of mixture components is increased up to $n = 10$ for smaller basic shapes (k-mers and objects (V3)), and up to $n = 5$ for other basic objects from table 1.

Example results for the time dependence of $\ln(\theta_J - \theta(t))$ are shown in figure 2 for the five-component mixtures containing various sizes of basic objects from table 1. For the late stages of the process these plots are straight lines, suggesting that the approach to the jamming limit is exponential in the form equation (1). Five sets of lines with different slopes are distinguished, corresponding to different numbers of possible object orientations $m = 1, 3, 8, 12$, and 24. The steepest slopes are obtained for the cubes (C8) having only one possible orientation, and they reach the jamming coverage for the shortest time. The process slows down with the number of possible object orientations, and it is the slowest for the objects without symmetry, having $m = 24$ possible orientations.

Values of the parameter σ (equation (1)) are determined from the slopes of the plots of $\ln(\theta_J - \theta(t))$ vs t in the late stage of the deposition process, and their dependence on the number of mixture components n is shown in figure 3. It can be seen that the value of the relaxation time σ increases linearly with the number of mixture components of the same basic shape. The values of the parameter σ are generally larger, and the relaxation time σ increases more sharply for the objects with a larger number of possible orientations m.

Plots of $\ln(\theta_J - \theta(t))$ vs t are shown in figure 4 for the five-component mixtures, and their components for k-mers, objects (P4), (V3), and (L4), having $m = 3, 8, 12$, and 24 possible orientations, respectively. In the late stages of the process these plots are straight lines not only for the mixtures but also for each of their components. This indicates that the approach to the jamming limit follows an exponential pattern for both the mixture and its components. Plots for the smallest mixture components align with those for the mixtures because the small unoccupied areas left at the end of the deposition process are mainly filled with the smallest components.

Dependence of the parameter σ on the size N of the mixture components for the ten-component mixtures of k-mers and for the ten-component mixtures of objects (V3)
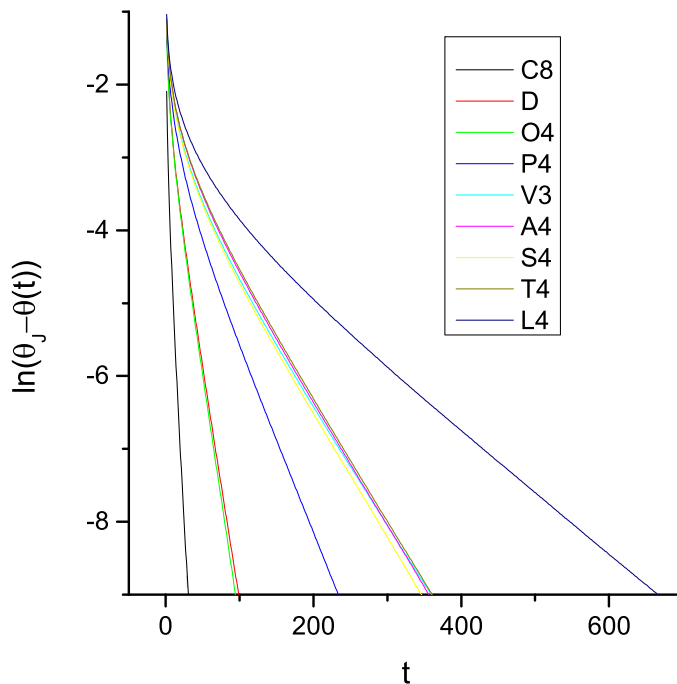
Figure 2. Plots of $\ln(\theta_{\mathrm{J}} - \theta(t))$ vs t for the five-component mixtures containing various sizes of basic objects: cubes (C8) with $m = 1$ orientation, (D), (O4) with $m = 3$ orientations, (P4) with $m = 8$ orientations, (V3), (A4), (S4), (T4) with $m = 12$ orientations, and (L4) with $m = 24$ orientations.

is shown in figure 5(a)). Similarly, this dependence is shown for the five-component mixtures of (L4), (P4), and (T4) in figure 5(b)). The relaxation time σ decreases rapidly with the size of the mixture components, so that at late times the kinetics of the deposition process is determined mostly by the smallest objects in the mixtures.

Jamming densities θ_{J} for the examined mixtures are presented in figure 6. Values of the jamming densities are determined up to ten-component mixtures for k-mers and for objects (V3), while for basic objects covering four lattice sites and for the cubes (C8) simulations are performed up to five-component mixtures. It is interesting to note that the jamming density of the mixture increases with the number of mixture components n, except for the objects (P4) and (S4). For most of the objects the jamming density increases despite the fact that the number of the mixture components is always increased by adding objects of a larger size. This increase is most prominent for mixtures of cubes.

During the RSA process leading to the jamming limit, each of the mixture components reaches its own jamming density. In order to gain a better insight into the deposit structure, partial jamming densities are determined and presented in figure 7. These partial jamming densities decrease with the object size N, and this decrease is more pronounced for smaller object sizes. Smaller objects fill the empty spaces left by the larger ones, and the smallest ones dominate in the final jamming configurations.

The smallest objects give the most significant contribution to the final jamming density. The difference in the behavior of the mixture jamming density for various object shapes can be understood by having this in mind. Larger objects leave areas of
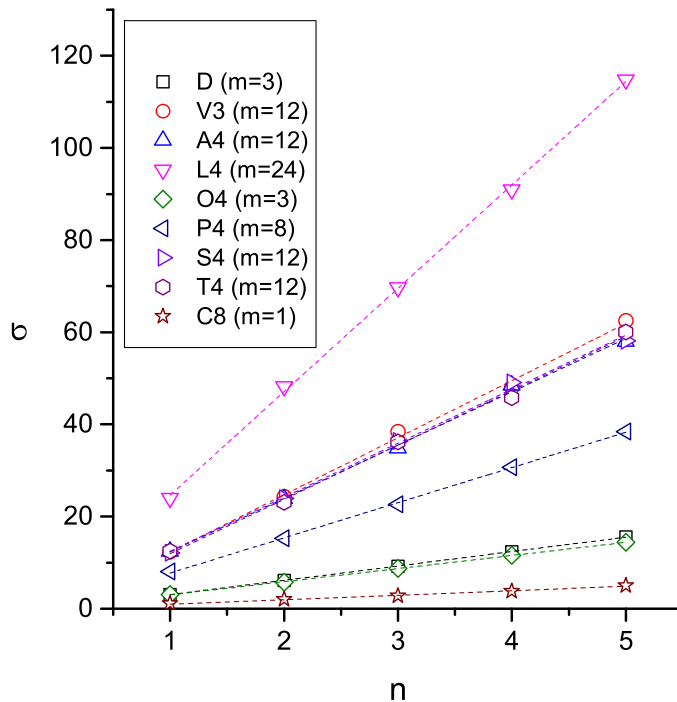
Figure 3. Dependence of the parameter σ (equation (1)) on the number of mixture components n for the five-component mixtures of basic objects from table 1. The number of mixture components n is always increased by adding an object of a larger size.

unoccupied sites that are filled with smaller ones. Final jamming density is predominantly determined by deposition of the smallest objects in the mixtures. Figure 8 shows the normalized partial jamming densities of the smallest objects for the n-component mixtures of various basic objects covering four lattice sites. These values are obtained by dividing the partial jamming density of the smallest object by the jamming density of the single basic shape. Results are shown for mixtures made of two, three, four, and five components. The difference between these normalized partial jamming densities increases with the number of mixture components n. Decrease is faster for the shapes (P4) and (S4), resulting in a reduction of the total jamming density with the number of mixture components.

An eight-component mixture of various shapes of the same size $N = 4$ is also examined. The kinetics of the deposition process is illustrated in figure 9 for the mixture and the mixture components. Four sets of lines with different slopes correspond to four different numbers of possible object orientations, $m = 3, 8, 12$, and 24. At late enough times, when the coverage fraction is sufficient to make the geometry of the unoccupied lattice site complex, the number of possible orientations m substantially influences the objects' adsorption rate. Objects with a lower number of possible orientations reach their partial jamming density in a shorter time. Consequently, in the late stage of the process, the kinetics of the mixture deposition is determined practically by the deposition of the component with the highest value of m. At late times, deposition events
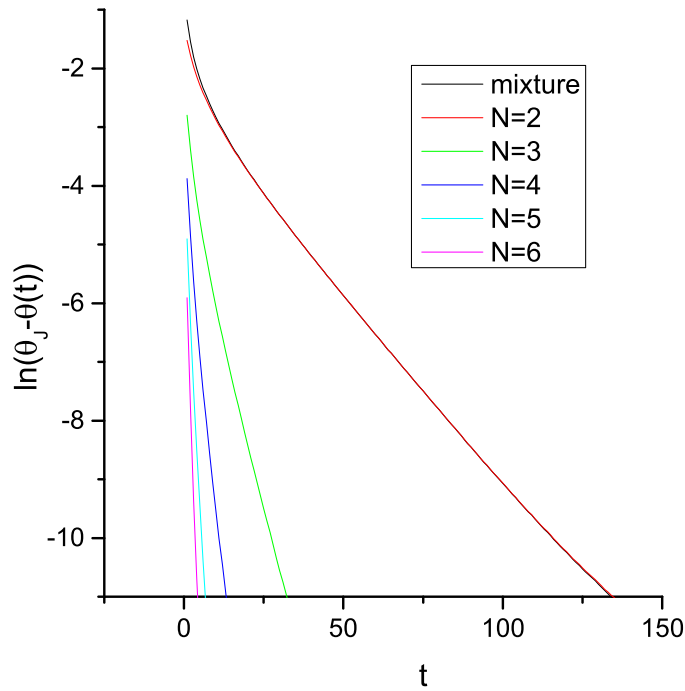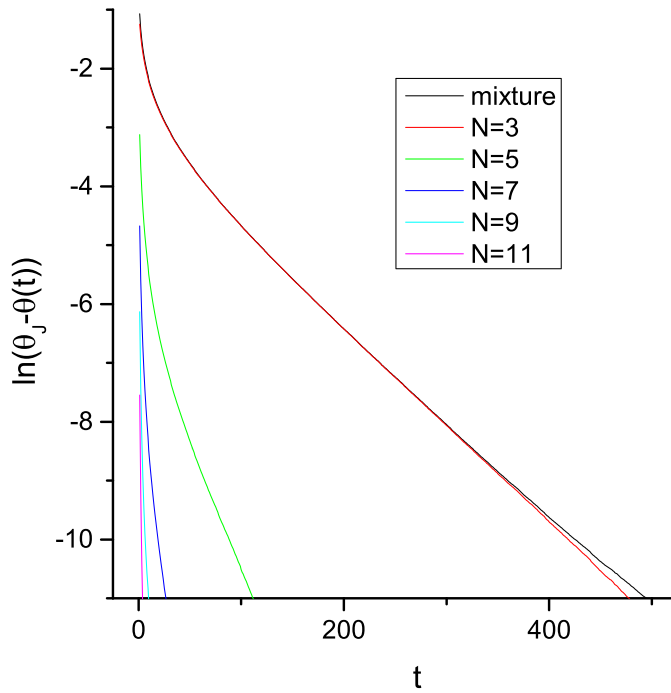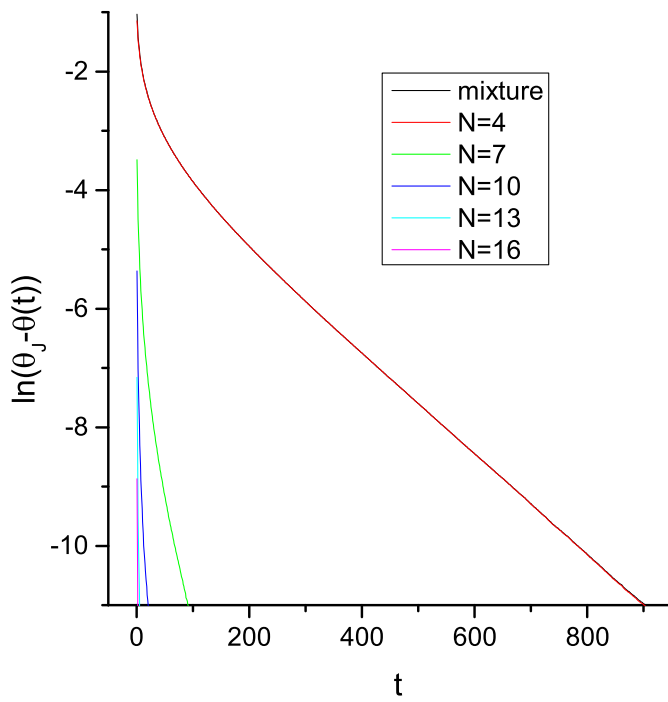
a)
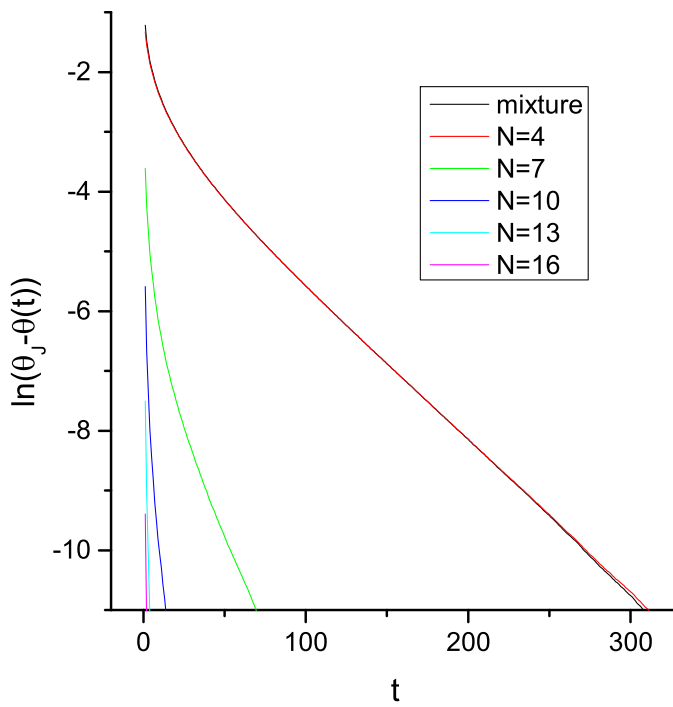
b)

Figure 4. Plots of $\ln(\theta_J - \theta(t))$ vs t for the five-component mixtures and their components. (a) k-mers with $m=3$ orientations; (b) objects of basic shape (P4) with $m=8$ orientations; (c) objects of basic shape (V3) with $m=12$ orientations; (d) objects of basic shape (L4) with $m=24$ orientations.
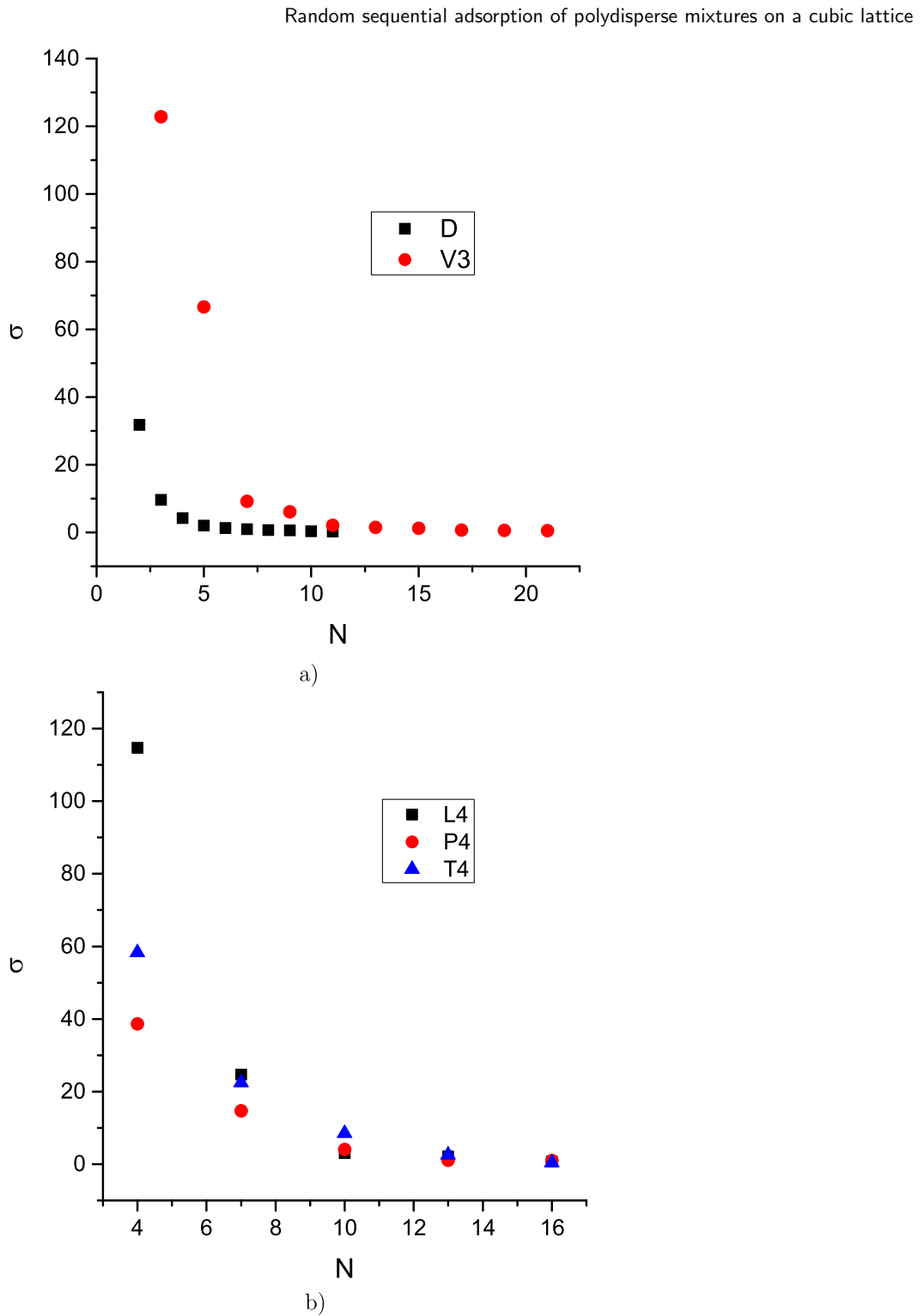
c)

d)

Figure 4. (Continued.)

Figure 5. Dependence of the parameter σ on the size N of the objects for the: (a) ten-component mixtures of objects (D) and (V3); (b) five-component mixtures of objects (L4), (P4), and (T4) from table 1.
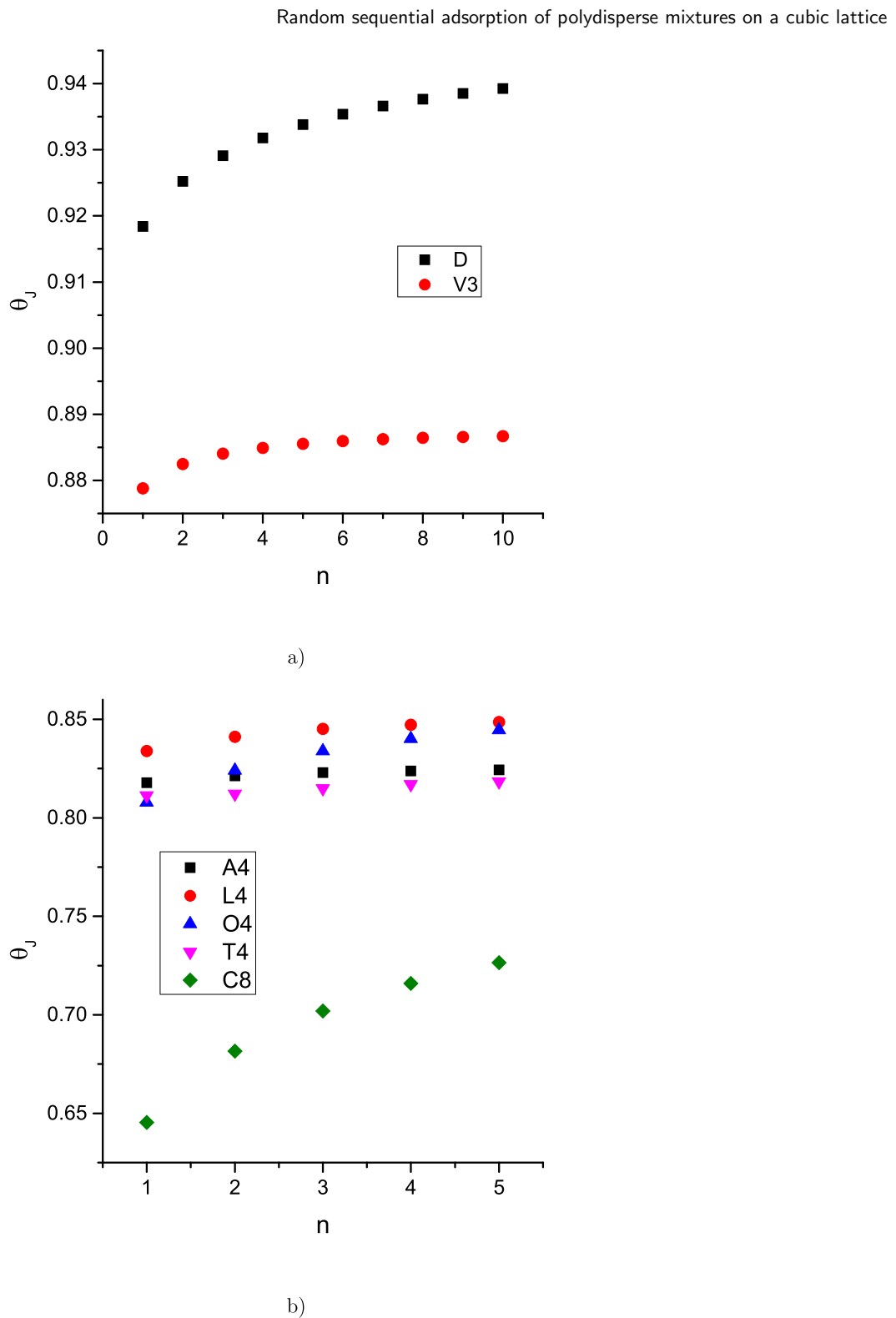
J. Stat. Mech. (2025) 013204

a)

b)

Figure 6. Dependence of the jamming density θ_J on the number of mixture components n for the mixtures of various sizes of basic shapes from table 1: (a) (D) and (V3); (b) (A4), (L4), (O4), (T4), and (C8); (c) (P4) and (S4). The number of components n is always increased by adding an object of a larger size.
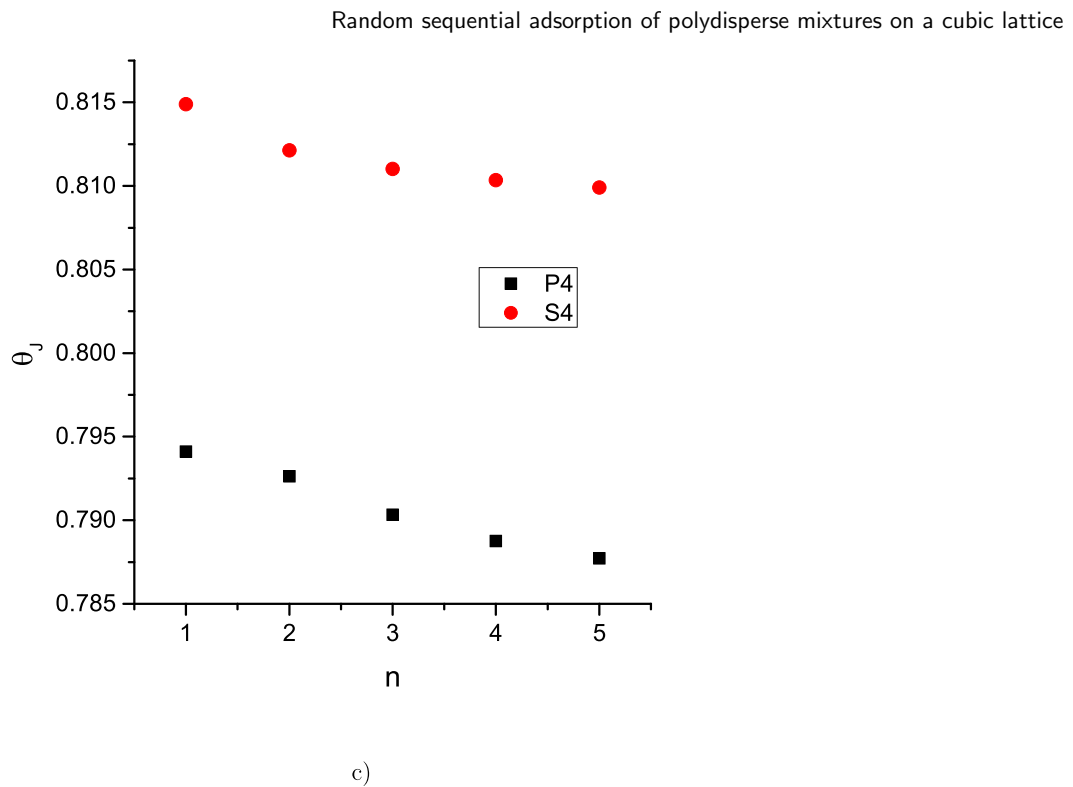
c)

Figure 6. (Continued.)

occur on small islands of unoccupied sites. There is only a restricted number of possible orientations in which an object can reach a vacant location, provided the location is small enough. For a shape with a larger number of possible orientations, it takes a longer time to examine all possible ways of placement in these small free areas. Values of the relaxation time σ and the jamming density θ_J for the eight-component mixture and for the mixture components are given in table 3.

Partial jamming densities of mixture components depend on their packing facilities with other objects. The number of possible orientations m is also one of the factors affecting the partial jamming density. The highest partial jamming density in the examined composite has the object (L4) with $m = 24$, and the lowest partial jamming densities are observed for the objects (P4) and (I4) with $m = 8$ and $m = 3$, respectively. Objects with larger m have enhanced abilities for filling the small empty regions left at late times of the process, which contributes to higher partial densities. A similar dependence of the jamming density on the number of possible orientations can be observed for the deposition of single objects [25], and for the two-component mixtures [39] on a three-dimensional cubic lattice. In the case of polydisperse mixtures, the relative difference in the jamming density of the object shapes with various numbers of possible orientations is even more pronounced.
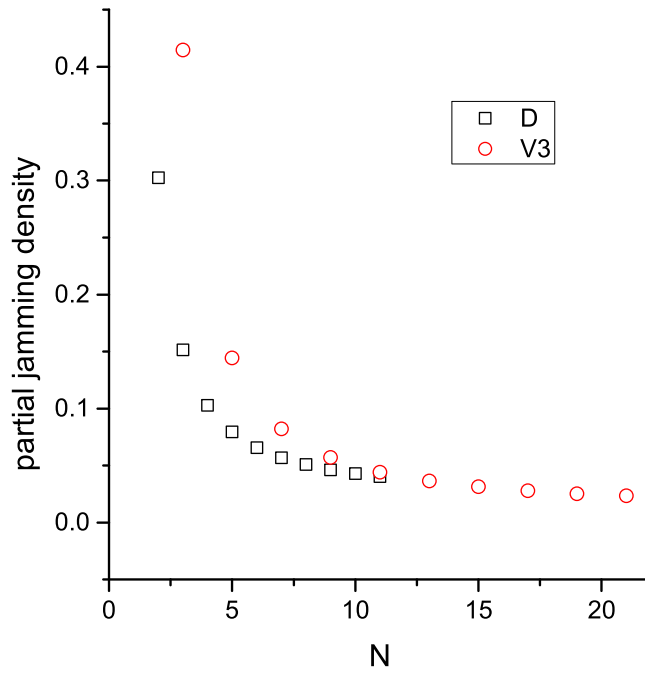
a)
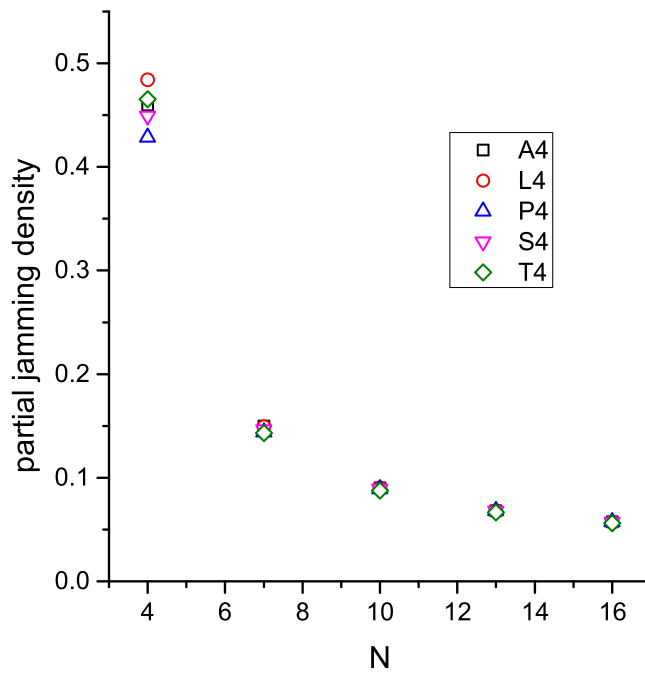
b)

Figure 7. Dependence of the partial jamming density on the component size N for the: (a) ten-component mixtures of objects (D) and (V3); (b) five-component mixtures of objects (A4), (L4), (P4), (S4), and (T4); (c) five-component mixtures of objects (O4); (d) five-component mixtures of objects (C8).
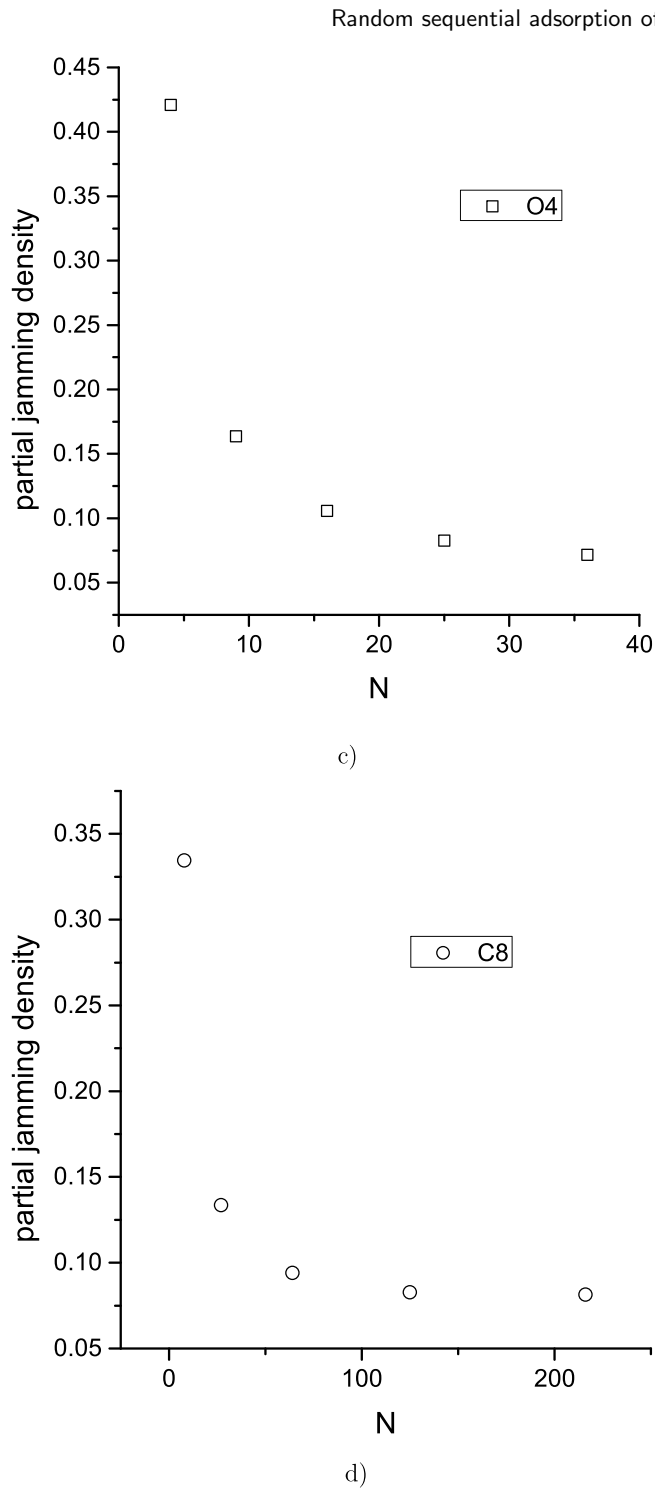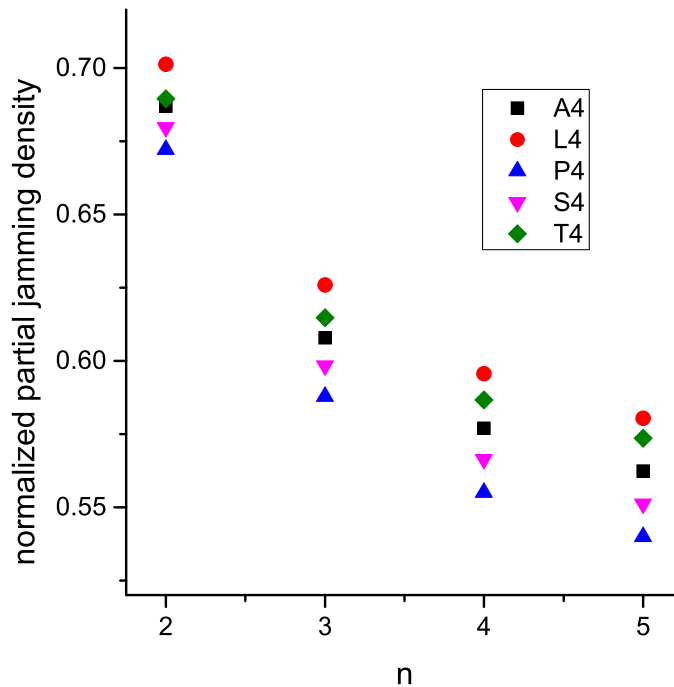
c)

d)

Figure 7. (Continued.)

Figure 8. Normalized partial jamming densities of the smallest objects for the n-component mixtures. These values are obtained by dividing the partial jamming density of the smallest object by the jamming density of the single basic shape.

4. Conclusion

We have performed extensive numerical simulations of the irreversible deposition of polydisperse mixtures composed of extended objects on a 3D cubic lattice. The impact of the geometric properties of the objects, as well as their polydispersity, on the kinetics of the deposition process has been studied.

We have analyzed polydisperse mixtures in which the size of shapes making the mixture gradually increases with the number of mixture components n. Basic shapes were all lattice animals covering two, three, and four lattice sites that can give different behavior, and a cube covering eight lattice sites. Special attention was paid to the dependence of the densification kinetics on the number of mixture components n. The deposition process slows down with the number of possible basic object orientations, and it is the slowest for the objects without symmetry. The relaxation time σ increases linearly with the number of mixture components of the same basic shape. For most objects the jamming density increases despite the fact that the number of mixture components is always increased by adding objects of a larger size. This behavior is predominantly determined by the ability of the smallest objects in the mixture to fill the small accessible areas left at late times of the process.

A similar effect was observed in the RSA of polydisperse mixtures on a triangular lattice [33]. In mixtures of more symmetrical shapes, such as line segments and triangles,
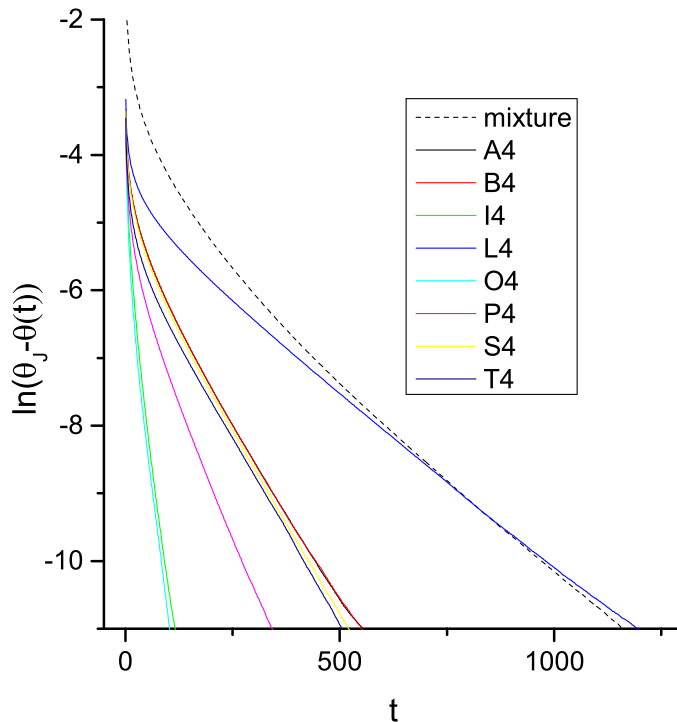
Figure 9. Plots of $\ln(\theta_J - \theta(t))$ vs t for the eight-component mixture of various objects covering $N = 4$ lattice sites. The plots are also shown for the mixture components, as indicated in the legend.

jamming coverage increases with the number of components. In contrast, mixtures of less symmetrical shapes exhibit a decrease in jamming coverage as n increases.

We have also performed a detailed analysis of the contribution to the densification kinetics coming from each mixture component. Both the partial jamming densities and the corresponding relaxation times decrease rapidly with the size of the objects making the mixture. Hence, the asymptotic behavior of the density is dominated by the smallest particles. For mixtures of lattice animals with different numbers of possible orientations m, but of the same number of segments, the relaxation time is smaller for components with lower m.

Acknowledgments

References

[1] Dabrowski A 2001 Adsorption-from theory to practice *Adv. Colloid Interface Sci.* **93** 135

[2] Donev A, Cisse I, Sachs D, Variano E A, Stillinger F H, Connelly R, Torquato S and Chaikin P M 2004 Improving the density of jammed disordered packings using ellipsoids *Science* **303** 990

[3] Cadilhe A, Araújo N A M and Privman V 2007 Random sequential adsorption: from continuum to lattice and pre-patterned substrates *J. Phys.: Condens. Matter* **19** 065124

[4] Liang J and Dill K A 2001 Are proteins well-packed? *Biophys. J.* **81** 751

[5] Purohit P K, Kondev J and Phillips R 2003 Mechanics of DNA packaging in viruses *Proc. Natl Acad. Sci. USA* **100** 3173

[6] Torquato S 2002 *Random Heterogeneous Materials: Microstructure and Macroscopic Properties* (Springer)

[7] Nagarajan R 2008 Nanoparticles: building blocks for nanotechnology. Nanoparticles: synthesis, stabilization, passivation and functionalization *ACS Symp. Ser.* **996** 2–14

[8] Vasudevan A, Shvalya V, Zidanšek A and Cvelbar U 2019 Tailoring electrical conductivity of two dimensional nanomaterials using plasma for edge electronics: a mini review *Front. Chem. Sci. Eng.* **13** 427

[9] Torquato S and Stillinger F H 2010 Jammed hard-particle packings: From Kepler to Bernal and beyond *Rev. Mod. Phys.* **82** 2633

[10] Evans J W 1993 Random and cooperative sequential adsorption *Rev. Mod. Phys.* **65** 1281

[11] Talbot J, Tarjus G, Van Tassel P R and Viot P 2000 From car parking to protein adsorption: an overview of sequential adsorption processes *Colloids Surf.* A **165** 287

[12] Ben-Naim E and Krapivsky P L 1994 On irreversible deposition on disordered substrates *J. Phys. A: Math. Gen.* **27** 3575

[13] Bonnier B 2001 Random sequential adsorption of binary mixtures on a line *Phys. Rev.* E **64** 066111

[14] Ciesla M and Barbasz J 2014 Random packing of regular polygons and star polygons on a flat two-dimensional surface *Phys. Rev.* E **90** 022402

[15] Manna S S and Švrakić N M 1991 Random sequential adsorption: line segments on the square lattice *J. Phys. A: Math. Gen.* **24** L671

[16] Budinski-Petković L, Lončarević I, Jakšić Z M, Vrhovac S B and Švrakić N M 2011 Simulation study of aniso-tropic random sequential adsorption of extended objects on a triangular lattice *Phys. Rev.* E **84** 051601

[17] Budinski-Petković L, Lončarević I, Jakšić Z M and Vrhovac S B 2016 Jamming and percolation in random sequen-tial adsorption of extended objects on a triangular lattice with quenched impurities *J. Stat. Mech.* 053101

[18] Aleksić B N, Švrakić N M and Belić M 2013 Kinetics of deposition of oriented superdisks *Phys. Rev.* E **88** 062112

[19] Ciesla M, Pajak G and Ziff R M 2016 In a search for a shape maximizing packing fraction for two-dimensional random sequential adsorption *J. Chem. Phys.* **145** 044708

[20] Kasperek W, Kubala P and Ciesla M 2018 Random sequential adsorption of unoriented rectangles at saturation *Phys. Rev.* E **98** 063310

[21] Ciesla M and Kubala P 2018 Random sequential adsorption of cubes *J. Chem. Phys.* **148** 024501

[22] Adamczyk P, Romiszowski P and Sikorski A 2008 A simple model of stiff and flexible polymer chain adsorption: the influence of the internal chain architecture *J. Chem. Phys.* **128** 154911

[23] Lebovka N I, Tarasevich Y Y, Dubinin D O, Laptev V V and Vygornitskii N V 2015 Jamming and percolation in generalized models of random sequential adsorption of linear k-mers on a square lattice *Phys. Rev.* E **92** 062116

[24] Budinski-Petković L, Lončarević I, Dujak D, Karač A, Šćepanović J R, Jakšić Z M and Vrhovac S B 2017 Particle morphology effects in random sequential adsorption *Phys. Rev.* E **95** 022114

[25] Lončarević I, Budinski-Petković L, Šćepanović J R, Jakšić Z M and Vrhovac S B 2020 Random sequential adsorption of lattice animals on a three-dimensional cubic lattice *Phys. Rev.* E **101** 012119

[26] Švrakić N M and Henkel M 1991 Kinetics of irreversible deposition of mixtures *J. Phys.* I **1** 791

[27] Subashiev A V and Luryi S 2007 Fluctuations of the partial filling factors in competitive random sequential adsorption from binary mixtures *Phys. Rev.* E **76** 011128

[28] Dias C S, Araújo N A M and Cadilhe A 2012 Analytical and numerical study of particles with binary adsorption *Phys. Rev.* E **85** 041120

[29] Dujak D, Karač A, Budinski-Petković L, Lončarević I, Jakšić Z M and Vrhovac S B 2019 Percolation in random sequential adsorption of mixtures on a triangular lattice *J. Stat. Mech.* 113210

[30] Adamczyk Z, Siwek B, Zembala M and Werónski P 1997 Influence of polydispersity on random sequential adsorption of spherical particles *J. Colloid Interface Sci.* **185** 236

[31] Vieira M C, Gomes M and de Lima J 2011 Effect of particle size distribution and dynamics on the performance of two-dimensional packing *Physica* A **390** 3404

[32] Marques J F, Lima A B, Araújo N A M and Cadilhe A 2012 Effect of particle polydispersity on the irreversible adsorption of fine particles on patterned substrates *Phys. Rev.* E **85** 061122

[33] Budinski-Petković L, Vrhovac S B and Lončarević I 2008 Random sequential adsorption of polydisperse mixtures on discrete substrates *Phys. Rev.* E **78** 061603

[34] Burridge D J 2010 Random packing of lines in a lattice cube *Phys. Rev.* E **81** 031107

[35] García G D, Sanchez-Varretti F O, Centres P M and Ramirez-Pastor A J 2015 Random sequential adsorption of straight rigid rods on a simple cubic lattice *Physica* A **436** 558

[36] Jensen I 2001 Enumerations of lattice animals and trees *J. Stat. Phys.* **102** 865

[37] Aleksandrowicz G and Barequet G 2009 Counting polycubes without the dimensionality curse *Discrete Math.* **309** 4576

[38] Lunnon W F 1972 Symmetry of cubical and general polyominoes *Graph Theory and Computing* ed C Ronald (Academic) pp 101–8

[39] Beljin-Čavić M, Lončarević I, Budinski-Petković L, Jakšić Z M and Vrhovac S B 2022 Simulation study of random sequential deposition of binary mixtures of lattice animals on a three-dimensional cubic lattice *J. Stat. Mech.* 053206